Evidence for the $\eta_b(1S)$ Meson in Radiative $\Upsilon(2S)$ Decay

B. Aubert,[1] M. Bona,[1] Y. Karyotakis,[1] J. P. Lees,[1] V. Poireau,[1] E. Prencipe,[1] X. Prudent,[1] V. Tisserand,[1]
J. Garra Tico,[2] E. Grauges,[2] L. Lopez[ab],[3] A. Palano[ab],[3] M. Pappagallo[ab],[3] G. Eigen,[4] B. Stugu,[4] L. Sun,[4]
M. Battaglia,[5] D. N. Brown,[5] L. T. Kerth,[5] Yu. G. Kolomensky,[5] G. Lynch,[5] I. L. Osipenkov,[5] K. Tackmann,[5]
T. Tanabe,[5] C. M. Hawkes,[6] N. Soni,[6] A. T. Watson,[6] H. Koch,[7] T. Schroeder,[7] D. J. Asgeirsson,[8] B. G. Fulsom,[8]
C. Hearty,[8] T. S. Mattison,[8] J. A. McKenna,[8] M. Barrett,[9] A. Khan,[9] A. Randle-Conde,[9] V. E. Blinov,[10]
A. D. Bukin,[10] A. R. Buzykaev,[10] V. P. Druzhinin,[10] V. B. Golubev,[10] A. P. Onuchin,[10] S. I. Serednyakov,[10]
Yu. I. Skovpen,[10] E. P. Solodov,[10] K. Yu. Todyshev,[10] M. Bondioli,[11] S. Curry,[11] I. Eschrich,[11] D. Kirkby,[11]
A. J. Lankford,[11] P. Lund,[11] M. Mandelkern,[11] E. C. Martin,[11] D. P. Stoker,[11] S. Abachi,[12] C. Buchanan,[12]
H. Atmacan,[13] J. W. Gary,[13] F. Liu,[13] O. Long,[13] G. M. Vitug,[13] Z. Yasin,[13] L. Zhang,[13] V. Sharma,[14]
C. Campagnari,[15] T. M. Hong,[15] D. Kovalskyi,[15] M. A. Mazur,[15] J. D. Richman,[15] T. W. Beck,[16] A. M. Eisner,[16]
C. A. Heusch,[16] J. Kroseberg,[16] W. S. Lockman,[16] A. J. Martinez,[16] T. Schalk,[16] B. A. Schumm,[16] A. Seiden,[16]
L. O. Winstrom,[16] C. H. Cheng,[17] D. A. Doll,[17] B. Echenard,[17] F. Fang,[17] D. G. Hitlin,[17] I. Narsky,[17]
T. Piatenko,[17] F. C. Porter,[17] R. Andreassen,[18] G. Mancinelli,[18] B. T. Meadows,[18] K. Mishra,[18] M. D. Sokoloff,[18]
P. C. Bloom,[19] W. T. Ford,[19] A. Gaz,[19] J. F. Hirschauer,[19] M. Nagel,[19] U. Nauenberg,[19] J. G. Smith,[19]
S. R. Wagner,[19] R. Ayad,[20, *] A. Soffer,[20, †] W. H. Toki,[20] R. J. Wilson,[20] E. Feltresi,[21] A. Hauke,[21] H. Jasper,[21]
M. Karbach,[21] J. Merkel,[21] A. Petzold,[21] B. Spaan,[21] K. Wacker,[21] M. J. Kobel,[22] R. Nogowski,[22] K. R. Schubert,[22]
R. Schwierz,[22] A. Volk,[22] D. Bernard,[23] G. R. Bonneaud,[23] E. Latour,[23] M. Verderi,[23] P. J. Clark,[24]
S. Playfer,[24] J. E. Watson,[24] M. Andreotti[ab],[25] D. Bettoni[a],[25] C. Bozzi[a],[25] R. Calabrese[ab],[25] A. Cecchi[ab],[25]
G. Cibinetto[ab],[25] P. Franchini[ab],[25] E. Luppi[ab],[25] M. Negrini[ab],[25] A. Petrella[ab],[25] L. Piemontese[a],[25] V. Santoro[ab],[25]
R. Baldini-Ferroli,[26] A. Calcaterra,[26] R. de Sangro,[26] G. Finocchiaro,[26] S. Pacetti,[26] P. Patteri,[26] I. M. Peruzzi,[26, ‡]
M. Piccolo,[26] M. Rama,[26] A. Zallo,[26] R. Contri[ab],[27] M. Lo Vetere[ab],[27] M. R. Monge[ab],[27] S. Passaggio[a],[27]
C. Patrignani[ab],[27] E. Robutti[a],[27] S. Tosi[ab],[27] K. S. Chaisanguanthum,[28] M. Morii,[28] A. Adametz,[29] J. Marks,[29]
S. Schenk,[29] U. Uwer,[29] F. U. Bernlochner,[30] V. Klose,[30] H. M. Lacker,[30] D. J. Bard,[31] P. D. Dauncey,[31]
M. Tibbetts,[31] P. K. Behera,[32] X. Chai,[32] M. J. Charles,[32] U. Mallik,[32] J. Cochran,[33] H. B. Crawley,[33] L. Dong,[33]
W. T. Meyer,[33] S. Prell,[33] E. I. Rosenberg,[33] A. E. Rubin,[33] Y. Y. Gao,[34] A. V. Gritsan,[34] Z. J. Guo,[34]
N. Arnaud,[35] J. Béquilleux,[35] A. D'Orazio,[35] M. Davier,[35] J. Firmino da Costa,[35] G. Grosdidier,[35]
F. Le Diberder,[35] V. Lepeltier,[35] A. M. Lutz,[35] S. Pruvot,[35] P. Roudeau,[35] M. H. Schune,[35] J. Serrano,[35]
V. Sordini,[35, §] A. Stocchi,[35] G. Wormser,[35] D. J. Lange,[36] D. M. Wright,[36] I. Bingham,[37] J. P. Burke,[37]
C. A. Chavez,[37] J. R. Fry,[37] E. Gabathuler,[37] R. Gamet,[37] D. E. Hutchcroft,[37] D. J. Payne,[37] C. Touramanis,[37]
A. J. Bevan,[38] C. K. Clarke,[38] F. Di Lodovico,[38] R. Sacco,[38] M. Sigamani,[38] G. Cowan,[39] S. Paramesvaran,[39]
A. C. Wren,[39] D. N. Brown,[40] C. L. Davis,[40] A. G. Denig,[41] M. Fritsch,[41] W. Gradl,[41] K. E. Alwyn,[42] D. Bailey,[42]
R. J. Barlow,[42] G. Jackson,[42] G. D. Lafferty,[42] T. J. West,[42] J. I. Yi,[42] J. Anderson,[43] C. Chen,[43] A. Jawahery,[43]
D. A. Roberts,[43] G. Simi,[43] J. M. Tuggle,[43] C. Dallapiccola,[44] E. Salvati,[44] S. Saremi,[44] R. Cowan,[45] D. Dujmic,[45]
P. H. Fisher,[45] S. W. Henderson,[45] G. Sciolla,[45] M. Spitznagel,[45] F. Taylor,[45] R. K. Yamamoto,[45] M. Zhao,[45]
P. M. Patel,[46] S. H. Robertson,[46] A. Lazzaro[ab],[47] V. Lombardo[a],[47] F. Palombo[ab],[47] J. M. Bauer,[48] L. Cremaldi,[48]
R. Godang,[48, ¶] R. Kroeger,[48] D. J. Summers,[48] H. W. Zhao,[48] M. Simard,[49] P. Taras,[49] H. Nicholson,[50]
G. De Nardo[ab],[51] L. Lista[a],[51] D. Monorchio[ab],[51] G. Onorato[ab],[51] C. Sciacca[ab],[51] G. Raven,[52] H. L. Snoek,[52]
C. P. Jessop,[53] K. J. Knoepfel,[53] J. M. LoSecco,[53] W. F. Wang,[53] L. A. Corwin,[54] K. Honscheid,[54] H. Kagan,[54]
R. Kass,[54] J. P. Morris,[54] A. M. Rahimi,[54] J. J. Regensburger,[54] S. J. Sekula,[54] Q. K. Wong,[54] N. L. Blount,[55]
J. Brau,[55] R. Frey,[55] O. Igonkina,[55] J. A. Kolb,[55] M. Lu,[55] R. Rahmat,[55] N. B. Sinev,[55] D. Strom,[55] J. Strube,[55]
E. Torrence,[55] G. Castelli[ab],[56] N. Gagliardi[ab],[56] M. Margoni[ab],[56] M. Morandin[a],[56] M. Posocco[a],[56] M. Rotondo[a],[56]
F. Simonetto[ab],[56] R. Stroili[ab],[56] C. Voci[ab],[56] P. del Amo Sanchez,[57] E. Ben-Haim,[57] H. Briand,[57] J. Chauveau,[57]
O. Hamon,[57] Ph. Leruste,[57] J. Ocariz,[57] A. Perez,[57] J. Prendki,[57] S. Sitt,[57] L. Gladney,[58] M. Biasini[ab],[59]
E. Manoni[ab],[59] C. Angelini[ab],[60] G. Batignani[ab],[60] S. Bettarini[ab],[60] G. Calderini[ab],[60, **] M. Carpinelli[ab],[60, ††]
A. Cervelli[ab],[60] F. Forti[ab],[60] M. A. Giorgi[ab],[60] A. Lusiani[ac],[60] G. Marchiori[ab],[60] M. Morganti[ab],[60] N. Neri[ab],[60]

E. Paoloni[ab],[60] G. Rizzo[ab],[60] J. J. Walsh[a],[60] D. Lopes Pegna,[61] C. Lu,[61] J. Olsen,[61] A. J. S. Smith,[61] A. V. Telnov,[61] F. Anulli[a],[62] E. Baracchini[ab],[62] G. Cavoto[a],[62] R. Faccini[ab],[62] F. Ferrarotto[a],[62] F. Ferroni[ab],[62] M. Gaspero[ab],[62] P. D. Jackson[a],[62] L. Li Gioi[a],[62] M. A. Mazzoni[a],[62] S. Morganti[a],[62] G. Piredda[a],[62] F. Renga[ab],[62] C. Voena[a],[62] M. Ebert,[63] T. Hartmann,[63] H. Schröder,[63] R. Waldi,[63] T. Adye,[64] B. Franek,[64] E. O. Olaiya,[64] F. F. Wilson,[64] S. Emery,[65] L. Esteve,[65] G. Hamel de Monchenault,[65] W. Kozanecki,[65] G. Vasseur,[65] Ch. Yèche,[65] M. Zito,[65] X. R. Chen,[66] H. Liu,[66] W. Park,[66] M. V. Purohit,[66] R. M. White,[66] J. R. Wilson,[66] M. T. Allen,[67] D. Aston,[67] R. Bartoldus,[67] J. F. Benitez,[67] R. Cenci,[67] J. P. Coleman,[67] M. R. Convery,[67] J. C. Dingfelder,[67] J. Dorfan,[67] G. P. Dubois-Felsmann,[67] W. Dunwoodie,[67] R. C. Field,[67] A. M. Gabareen,[67] M. T. Graham,[67] P. Grenier,[67] C. Hast,[67] W. R. Innes,[67] J. Kaminski,[67] M. H. Kelsey,[67] H. Kim,[67] P. Kim,[67] M. L. Kocian,[67] D. W. G. S. Leith,[67] S. Li,[67] B. Lindquist,[67] S. Luitz,[67] V. Luth,[67] H. L. Lynch,[67] D. B. MacFarlane,[67] H. Marsiske,[67] R. Messner,[67] D. R. Muller,[67] H. Neal,[67] S. Nelson,[67] C. P. O'Grady,[67] I. Ofte,[67] M. Perl,[67] B. N. Ratcliff,[67] A. Roodman,[67] A. A. Salnikov,[67] R. H. Schindler,[67] J. Schwiening,[67] A. Snyder,[67] D. Su,[67] M. K. Sullivan,[67] K. Suzuki,[67] S. K. Swain,[67] J. M. Thompson,[67] J. Va'vra,[67] A. P. Wagner,[67] M. Weaver,[67] C. A. West,[67] W. J. Wisniewski,[67] M. Wittgen,[67] D. H. Wright,[67] H. W. Wulsin,[67] A. K. Yarritu,[67] K. Yi,[67] C. C. Young,[67] V. Ziegler,[67] P. R. Burchat,[68] A. J. Edwards,[68] T. S. Miyashita,[68] S. Ahmed,[69] M. S. Alam,[69] J. A. Ernst,[69] B. Pan,[69] M. A. Saeed,[69] S. B. Zain,[69] S. M. Spanier,[70] B. J. Wogsland,[70] R. Eckmann,[71] J. L. Ritchie,[71] A. M. Ruland,[71] C. J. Schilling,[71] R. F. Schwitters,[71] B. W. Drummond,[72] J. M. Izen,[72] X. C. Lou,[72] F. Bianchi[ab],[73] D. Gamba[ab],[73] M. Pelliccioni[ab],[73] M. Bomben[ab],[74] L. Bosisio[ab],[74] C. Cartaro[ab],[74] G. Della Ricca[ab],[74] L. Lanceri[ab],[74] L. Vitale[ab],[74] V. Azzolini,[75] N. Lopez-March,[75] F. Martinez-Vidal,[75] D. A. Milanes,[75] A. Oyanguren,[75] J. Albert,[76] Sw. Banerjee,[76] B. Bhuyan,[76] H. H. F. Choi,[76] K. Hamano,[76] G. J. King,[76] R. Kowalewski,[76] M. J. Lewczuk,[76] I. M. Nugent,[76] J. M. Roney,[76] R. J. Sobie,[76] T. J. Gershon,[77] P. F. Harrison,[77] J. Ilic,[77] T. E. Latham,[77] G. B. Mohanty,[77] E. M. T. Puccio,[77] H. R. Band,[78] X. Chen,[78] S. Dasu,[78] K. T. Flood,[78] Y. Pan,[78] R. Prepost,[78] C. O. Vuosalo,[78] and S. L. Wu[78]

(The *BABAR* Collaboration)

[1]*Laboratoire de Physique des Particules, IN2P3/CNRS et Université de Savoie, F-74941 Annecy-Le-Vieux, France*
[2]*Universitat de Barcelona, Facultat de Fisica, Departament ECM, E-08028 Barcelona, Spain*
[3]*INFN Sezione di Bari[a]; Dipartmento di Fisica, Università di Bari[b], I-70126 Bari, Italy*
[4]*University of Bergen, Institute of Physics, N-5007 Bergen, Norway*
[5]*Lawrence Berkeley National Laboratory and University of California, Berkeley, California 94720, USA*
[6]*University of Birmingham, Birmingham, B15 2TT, United Kingdom*
[7]*Ruhr Universität Bochum, Institut für Experimentalphysik 1, D-44780 Bochum, Germany*
[8]*University of British Columbia, Vancouver, British Columbia, Canada V6T 1Z1*
[9]*Brunel University, Uxbridge, Middlesex UB8 3PH, United Kingdom*
[10]*Budker Institute of Nuclear Physics, Novosibirsk 630090, Russia*
[11]*University of California at Irvine, Irvine, California 92697, USA*
[12]*University of California at Los Angeles, Los Angeles, California 90024, USA*
[13]*University of California at Riverside, Riverside, California 92521, USA*
[14]*University of California at San Diego, La Jolla, California 92093, USA*
[15]*University of California at Santa Barbara, Santa Barbara, California 93106, USA*
[16]*University of California at Santa Cruz, Institute for Particle Physics, Santa Cruz, California 95064, USA*
[17]*California Institute of Technology, Pasadena, California 91125, USA*
[18]*University of Cincinnati, Cincinnati, Ohio 45221, USA*
[19]*University of Colorado, Boulder, Colorado 80309, USA*
[20]*Colorado State University, Fort Collins, Colorado 80523, USA*
[21]*Technische Universität Dortmund, Fakultät Physik, D-44221 Dortmund, Germany*
[22]*Technische Universität Dresden, Institut für Kern- und Teilchenphysik, D-01062 Dresden, Germany*
[23]*Laboratoire Leprince-Ringuet, CNRS/IN2P3, Ecole Polytechnique, F-91128 Palaiseau, France*
[24]*University of Edinburgh, Edinburgh EH9 3JZ, United Kingdom*
[25]*INFN Sezione di Ferrara[a]; Dipartimento di Fisica, Università di Ferrara[b], I-44100 Ferrara, Italy*
[26]*INFN Laboratori Nazionali di Frascati, I-00044 Frascati, Italy*
[27]*INFN Sezione di Genova[a]; Dipartimento di Fisica, Università di Genova[b], I-16146 Genova, Italy*
[28]*Harvard University, Cambridge, Massachusetts 02138, USA*
[29]*Universität Heidelberg, Physikalisches Institut, Philosophenweg 12, D-69120 Heidelberg, Germany*
[30]*Humboldt-Universität zu Berlin, Institut für Physik, Newtonstr. 15, D-12489 Berlin, Germany*
[31]*Imperial College London, London, SW7 2AZ, United Kingdom*
[32]*University of Iowa, Iowa City, Iowa 52242, USA*
[33]*Iowa State University, Ames, Iowa 50011-3160, USA*
[34]*Johns Hopkins University, Baltimore, Maryland 21218, USA*

[35]*Laboratoire de l'Accélérateur Linéaire, IN2P3/CNRS et Université Paris-Sud 11,*
Centre Scientifique d'Orsay, B. P. 34, F-91898 Orsay Cedex, France
[36]*Lawrence Livermore National Laboratory, Livermore, California 94550, USA*
[37]*University of Liverpool, Liverpool L69 7ZE, United Kingdom*
[38]*Queen Mary, University of London, London, E1 4NS, United Kingdom*
[39]*University of London, Royal Holloway and Bedford New College, Egham, Surrey TW20 0EX, United Kingdom*
[40]*University of Louisville, Louisville, Kentucky 40292, USA*
[41]*Johannes Gutenberg-Universität Mainz, Institut für Kernphysik, D-55099 Mainz, Germany*
[42]*University of Manchester, Manchester M13 9PL, United Kingdom*
[43]*University of Maryland, College Park, Maryland 20742, USA*
[44]*University of Massachusetts, Amherst, Massachusetts 01003, USA*
[45]*Massachusetts Institute of Technology, Laboratory for Nuclear Science, Cambridge, Massachusetts 02139, USA*
[46]*McGill University, Montréal, Québec, Canada H3A 2T8*
[47]*INFN Sezione di Milano[a]; Dipartimento di Fisica, Università di Milano[b], I-20133 Milano, Italy*
[48]*University of Mississippi, University, Mississippi 38677, USA*
[49]*Université de Montréal, Physique des Particules, Montréal, Québec, Canada H3C 3J7*
[50]*Mount Holyoke College, South Hadley, Massachusetts 01075, USA*
[51]*INFN Sezione di Napoli[a]; Dipartimento di Scienze Fisiche,*
Università di Napoli Federico II[b], I-80126 Napoli, Italy
[52]*NIKHEF, National Institute for Nuclear Physics and High Energy Physics, NL-1009 DB Amsterdam, The Netherlands*
[53]*University of Notre Dame, Notre Dame, Indiana 46556, USA*
[54]*Ohio State University, Columbus, Ohio 43210, USA*
[55]*University of Oregon, Eugene, Oregon 97403, USA*
[56]*INFN Sezione di Padova[a]; Dipartimento di Fisica, Università di Padova[b], I-35131 Padova, Italy*
[57]*Laboratoire de Physique Nucléaire et de Hautes Energies,*
IN2P3/CNRS, Université Pierre et Marie Curie-Paris6,
Université Denis Diderot-Paris7, F-75252 Paris, France
[58]*University of Pennsylvania, Philadelphia, Pennsylvania 19104, USA*
[59]*INFN Sezione di Perugia[a]; Dipartimento di Fisica, Università di Perugia[b], I-06100 Perugia, Italy*
[60]*INFN Sezione di Pisa[a]; Dipartimento di Fisica,*
Università di Pisa[b]; Scuola Normale Superiore di Pisa[c], I-56127 Pisa, Italy
[61]*Princeton University, Princeton, New Jersey 08544, USA*
[62]*INFN Sezione di Roma[a]; Dipartimento di Fisica,*
Università di Roma La Sapienza[b], I-00185 Roma, Italy
[63]*Universität Rostock, D-18051 Rostock, Germany*
[64]*Rutherford Appleton Laboratory, Chilton, Didcot, Oxon, OX11 0QX, United Kingdom*
[65]*CEA, Irfu, SPP, Centre de Saclay, F-91191 Gif-sur-Yvette, France*
[66]*University of South Carolina, Columbia, South Carolina 29208, USA*
[67]*SLAC National Accelerator Laboratory, Stanford, CA 94309, USA*
[68]*Stanford University, Stanford, California 94305-4060, USA*
[69]*State University of New York, Albany, New York 12222, USA*
[70]*University of Tennessee, Knoxville, Tennessee 37996, USA*
[71]*University of Texas at Austin, Austin, Texas 78712, USA*
[72]*University of Texas at Dallas, Richardson, Texas 75083, USA*
[73]*INFN Sezione di Torino[a]; Dipartimento di Fisica Sperimentale, Università di Torino[b], I-10125 Torino, Italy*
[74]*INFN Sezione di Trieste[a]; Dipartimento di Fisica, Università di Trieste[b], I-34127 Trieste, Italy*
[75]*IFIC, Universitat de Valencia-CSIC, E-46071 Valencia, Spain*
[76]*University of Victoria, Victoria, British Columbia, Canada V8W 3P6*
[77]*Department of Physics, University of Warwick, Coventry CV4 7AL, United Kingdom*
[78]*University of Wisconsin, Madison, Wisconsin 53706, USA*
(Dated: October 19, 2009)

We have performed a search for the $\eta_b(1S)$ meson in the radiative decay of the $\Upsilon(2S)$ resonance using a sample of 91.6×10^6 $\Upsilon(2S)$ events recorded with the *BABAR* detector at the PEP-II B factory at the SLAC National Accelerator Laboratory. We observe a peak in the photon energy spectrum at $E_\gamma = 609.3^{+4.6}_{-4.5}(\text{stat}) \pm 1.9(\text{syst})$ MeV, corresponding to an $\eta_b(1S)$ mass of $9394.2^{+4.8}_{-4.9}(\text{stat}) \pm 2.0(\text{syst})$ MeV/c^2. The branching fraction for the decay $\Upsilon(2S) \to \gamma\eta_b(1S)$ is determined to be $[3.9 \pm 1.1(\text{stat})^{+1.1}_{-0.9}(\text{syst})] \times 10^{-4}$. We find the ratio of branching fractions $\mathcal{B}[\Upsilon(2S) \to \gamma\eta_b(1S)]/\mathcal{B}[\Upsilon(3S) \to \gamma\eta_b(1S)] = 0.82 \pm 0.24(\text{stat})^{+0.20}_{-0.19}(\text{syst})$.

PACS numbers: 13.20.Gd, 14.40.Gx, 14.65.Fy

A candidate for the $\eta_b(1S)$ meson, the ground state of   the bottomonium system, was recently observed in the

radiative decays of the $\Upsilon(3S)$ [1]. The BABAR experiment has accumulated a large sample of data at the peak of the $\Upsilon(2S)$ resonance, where radiative $\Upsilon(2S)$ decays are also expected to produce the $\eta_b(1S)$ meson. Theoretical predictions for $\mathcal{B}[\Upsilon(2S) \to \gamma\eta_b(1S)]$ range from $(1-15) \times 10^{-4}$ [2]. A 90% confidence level upper limit of $\mathcal{B}[\Upsilon(2S) \to \gamma\,\eta_b(1S)] < 5.1 \times 10^{-4}$ is provided by the CLEO III experiment [3].

The ratio of branching fractions for the transitions $\Upsilon(2S) \to \gamma\eta_b(1S)$ and $\Upsilon(3S) \to \gamma\eta_b(1S)$ is dependent upon the overlap integrals of the relevant bottomonium wave functions [2], enabling a test that the observed state is the $\eta_b(1S)$ meson. More generally, the measured hyperfine mass splitting between the triplet and singlet states in the bottomonium system provides a better understanding of nonrelativistic bound states in QCD and the role of spin-spin interactions in quarkonium models [4, 5].

In this Letter, we report evidence for the radiative transition $\Upsilon(2S) \to \gamma\,\eta_b(1S)$. Hereafter $\eta_b(1S)$ will be abbreviated as η_b.

The data used in this analysis were collected with the BABAR detector [6] at the PEP-II asymmetric-energy e^+e^- storage rings. The primary data sample consists of 14 fb^{-1} of integrated luminosity collected at the peak of the $\Upsilon(2S)$ resonance. An additional sample of 44 fb^{-1} collected 40 MeV below the $\Upsilon(4S)$ resonance is used for background and efficiency studies. The trajectories of charged particles are reconstructed with a combination of five layers of double-sided silicon strip detectors and a 40-layer drift chamber, both operated in the 1.5-T magnetic field of a superconducting solenoid. Photons are detected with a CsI(Tl) electromagnetic calorimeter (EMC). The photon energy resolution varies from 3.4% (at 300 MeV) to 2.8% (at 800 MeV). Hereafter we quote values of E_γ measured in the center-of-mass (c.m.) frame.

The signal for $\Upsilon(2S) \to \gamma\,\eta_b$ is extracted from a fit to the inclusive photon energy spectrum. The monochromatic photon from this decay should appear as a peak in the photon energy spectrum near 615 MeV on top of a smooth nonpeaking background from continuum ($e^+e^- \to q\bar{q}$ with $q = u, d, s, c$) events and bottomonium decays.

Two other processes produce peaks in the photon energy spectrum close to the signal region: ISR production of the $\Upsilon(1S)$ and double radiative decays of the $\Upsilon(2S)$. The second transition in the processes $\Upsilon(2S) \to \gamma\chi_{bJ}(1P), \chi_{bJ}(1P) \to \gamma\Upsilon(1S)$, $J = 0, 1, 2$, produces peaks centered at 391, 423, and 442 MeV, respectively. These three peaks are merged due to photon energy resolution and the small Doppler broadening that arises from the motion of the $\chi_{bJ}(1P)$ in the c.m. frame. We use the $\chi_{bJ}(1P) \to \gamma\Upsilon(1S)$ signal to validate estimates of signal efficiencies and determine the absolute photon energy scale. Radiative production of the $\Upsilon(1S)$ via initial state radiation (ISR), $e^+e^- \to \gamma_{ISR}\Upsilon(1S)$, leads to a peak near 550 MeV. The signal peak is better separated from the peaking background, with respect to the $\Upsilon(3S) \to \gamma\eta_b$ analysis [1], primarily due to better absolute energy resolution at lower energy.

Decays of the η_b via two gluons, expected to be its dominant decay mode, have high charged-particle multiplicity. We select hadronic events by requiring four or more charged tracks in the event and that the ratio of the second to zeroth Fox-Wolfram moments [7] be less than 0.98.

Photon candidates are required to be isolated from all charged tracks. To ensure that their EMC shapes are consistent with an electromagnetic shower, the lateral moment [8] is required to be less than 0.55. To ensure high reconstruction efficiency and good energy resolution, the signal photon candidate is required to lie in the central angular region of the EMC, $-0.762 < \cos(\theta_{\gamma,\mathrm{LAB}}) < 0.890$, where $\theta_{\gamma,\mathrm{LAB}}$ is the angle between the photon and the beam axis in the laboratory frame.

The correlation of the direction of the photon with the thrust axis [9] of the η_b is small, as there is no preferred direction in the decay of the spin-zero η_b and the momentum of the η_b is small in the c.m. frame. In contrast, there is a strong correlation between the photon direction and thrust axis in continuum events. The thrust axis is computed with all charged tracks and neutral calorimeter clusters in the event, with the exception of the signal photon candidate. A requirement of $|\cos\theta_T| < 0.8$ is made to reduce continuum background, where θ_T is the angle between the thrust axis and the momentum of the signal photon candidate.

A principle source of background is photons from π^0 decays. A signal photon candidate is rejected if in combination with another photon in the event it forms a π^0 candidate whose mass is within 15 MeV/c^2 of the nominal π^0 mass. To maintain high signal efficiency, we require the second photon of the π^0 candidate to have an energy in the laboratory frame greater than 40 MeV.

The final efficiency evaluated from simulated events is 35.8%.

The selection criteria were chosen by maximizing the ratio $N_S/\sqrt{N_T}$, where N_S is the signal yield and N_T is the total yield of events in the signal region. The result of the optimization is insensitive to the exact definition of the signal region. A detailed Monte Carlo (MC) simulation [10] provides the signal sample for this optimization, while a small fraction (7%) of the $\Upsilon(2S)$ data is used to model the background. To avoid a potential bias, these data are excluded from the final fit of the photon energy spectrum. The remaining $\Upsilon(2S)$ data used for the analysis have an integrated luminosity of 13 fb^{-1}, corresponding to (91.6 ± 0.9) million $\Upsilon(2S)$ events.

To extract the η_b signal, a χ^2 fit of the E_γ spectrum is performed in the region $0.27 < E_\gamma < 0.80$ GeV. The fit includes four components: nonpeaking background, $\chi_{bJ}(1P) \to \gamma\Upsilon(1S)$, $\gamma_{ISR}\Upsilon(1S)$, and the η_b signal.

The nonpeaking background is parametrized by an empirical probability density function (PDF) $A \exp\left(\sum_{i=1}^{4} c_i x^i\right)$, where $x = E_\gamma$, and A, c_i are determined in the fit.

Doppler-broadened Crystal Ball (CB) functions [11] are used as phenomenological PDFs for the three $\chi_{bJ}(1P) \to \gamma\Upsilon(1S)$ shapes. The CB function is a Gaussian modified to have an extended power-law tail on the low (left) side. The power law parameter describing the low-side tail of the CB function is common to all three of the $\chi_{bJ}(1P)$ peaks. The Doppler broadening of the $\chi_{bJ}(1P)$ peaks is modeled by analytically convolving the CB functions with rectangular functions of half-width 6.5, 5.5, and 4.9 MeV for the $J = 0, 1, 2$ states, respectively. These values are evaluated using the $\Upsilon(2S)$ and $\chi_{bJ}(1P)$ masses [12]. The resolution parameter of the $\chi_{b0}(1P)$ PDF is fixed to that of the $\chi_{b2}(1P)$. Due to its small yield and its position on the low side of the $\chi_{bJ}(1P)$ peak, the exact width of the $\chi_{b0}(1P)$ is not crucial. The relative rates of the $\chi_{bJ}(1P)$ components are fixed to values determined from a control sample of $\Upsilon(2S) \to \gamma\chi_{bJ}(1P), \chi_{bJ}(1P) \to \gamma\Upsilon(1S), \Upsilon(1S) \to \mu^+\mu^-$ events, and the relative peak positions from the world-averaged (PDG) values [12], with a photon energy scale offset determined in the fit.

The PDF of the peaking background from ISR $\Upsilon(1S)$ production is parametrized as a CB function with parameters determined from simulated events. The ISR peak position is fixed to the value determined by the $\Upsilon(1S)$ and $\Upsilon(2S)$ masses [12], minus the energy scale offset shared with the $\chi_{bJ}(1P)$ peaks.

The η_b signal PDF is a nonrelativistic Breit-Wigner function convolved with a CB function to account for the experimental E_γ resolution. The CB parameters are determined from signal MC. Theoretical predictions for the η_b width, based on the expected ratio of the two-photon and two-gluon widths, range from 4 to 20 MeV [13]. Since the width of the η_b is not known, we have chosen a nominal value of 10 MeV, as in the $\Upsilon(3S)$ analysis.

The free parameters in the fit are the normalizations of all fit components, all of the nonpeaking background PDF parameters, the η_b peak position, the energy scale offset, the $\chi_{b1}(1P)$ and $\chi_{b2}(1P)$ CB resolutions, and the transition point between the Gaussian and power law components of the $\chi_{bJ}(1P)$ CB functions.

Figure 1 shows the photon energy spectrum and the fit result before (a) and after (b) subtraction of the nonpeaking background. The χ^2 per degree of freedom from the fit is 115/93. The line shapes of the three peaking components, $\chi_{bJ}(1P)$, ISR $\Upsilon(1S)$, and the η_b signal, are clearly visible in the subtracted spectrum. The η_b signal yield is 12800 ± 3500 events, and the η_b peak energy is $607.9^{+4.6}_{-4.5}$ MeV. The observed signal width is consistent with being dominated by the resolution of 18 MeV.

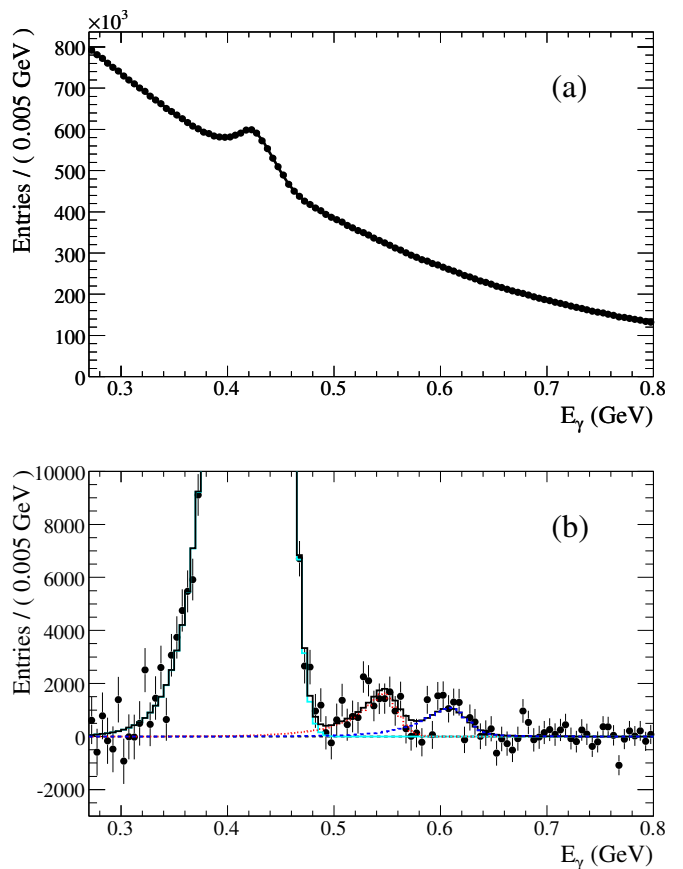The ISR $\Upsilon(1S)$ yield can be estimated from data col-

FIG. 1: (a) Inclusive photon spectrum in the region $0.27 < E_\gamma < 0.80$ GeV. The fit is overlaid on the data points. (b) (color online) Inclusive photon spectrum after subtracting the nonpeaking background, with the PDFs for $\chi_{bJ}(1P)$ peak (light solid line), ISR $\Upsilon(1S)$ (dotted line), η_b signal (dashed line) and the sum of all three (dark solid line).

lected below the $\Upsilon(4S)$ resonance. After correcting for the luminosity ratio, and the difference in ISR cross section and detection efficiencies at the two energies, we expect $16700 \pm 700 \pm 1200$ ISR $\Upsilon(1S)$ events in the on-resonance $\Upsilon(2S)$ data sample. The consistency of the observed yield of the $\Upsilon(1S)$ component, 16800^{+4200}_{-4000} events, with the expected value provides an important validation of the fitted background rate near the signal region. The yield and peak position of the η_b signal change by less than 0.1σ when the ISR $\Upsilon(1S)$ yield is fixed to the expected value.

We estimate the systematic uncertainty by varying the Breit-Wigner width in the η_b PDF to 5, 15, and 20 MeV, varying the PDF parameters fixed in the fit by $\pm 1\,\sigma$, using alternative smooth background shapes, varying the histogram binning between 1 and 15 MeV, incorporating a high-side tail to the $\chi_{bJ}(1P)$ peaks, and subtracting possible peaking background components. Smooth background PDF variations consist of using al-

ternative smooth background shapes that either incorporate a 3rd-order polynomial in the exponential (i.e. $c_4 = 0$) or use a PDF of the form $k \left(E_\gamma/E_0\right)^{-\Gamma_1} [1 + (E_\gamma/E_0)^{1/\alpha}]^{-(\Gamma_2-\Gamma_1)\alpha}$. Other background shape variations consisting of adding a term $c_5 x^5$ to the exponential of the smooth background function or adding a constant background PDF were found to change the fit negligibly. An additional high-side tail in the $\chi_{bJ}(1P)$ peak may be produced by the coincidental overlap of photons from $\chi_{bJ}(1P)$ decays with particles from the rest of the event or beam debris. We model this tail as a 90 MeV wide Gaussian centered about each of the $\chi_{bJ}(1P)$ peaks. Due to the large width of this component, it is indistinguishable from the nonpeaking background, and its inclusion does not improve the fit. We take the difference between the nominal fit and the fit including this tail as a systematic error. To evaluate the systematic due to the $\chi_{b0}(1P)$ resolution, we perform a fit in which the $\chi_{b0}(1P)$ resolution is fixed to that of the $J = 1$ state. To investigate the possible effect of peaking background from $\Upsilon(2S) \to (\pi^0, \eta)\Upsilon(1S)$ events, these contributions are subtracted prior to fitting, assuming the measured value and 90% CL upper limits for the branching fraction of the η and π^0 [12] transitions, respectively, giving a variation of -71 $(+651)$ events for the η (π^0) transition. Photons from the transition $\Upsilon(2S) \to \pi^0\pi^0\Upsilon(1S)$, which produce a smoothly varying background below 400 MeV, are absorbed into the smooth background PDF and do not require a separate systematic error.

Including systematic uncertainties, the signal yield is $12800 \pm 3500^{+3500}_{-3100}$ events. The largest contributions to the systematic error on the η_b yield are from the η_b width variation ($^{+1700}_{-1200}$ events) and the background shape variation ($^{+2600}_{-2700}$ events).

The photon energy scale is corrected with the fitted energy scale offset of $1.4 \pm 0.2 \pm 0.7$ MeV determined from the $\chi_{bJ}(1P)$ and ISR peaks. The systematic error is half of the shift added in quadrature with the PDG errors on the $\chi_{bJ}(1P)$ masses (0.4 MeV). The ISR peak contributes negligibly to the determination of the offset, due to its small yield. After including an additional systematic uncertainty of 1.7 MeV from the fit variations described above, we obtain a value of $E_\gamma = 609.3^{+4.6}_{-4.5} \pm 1.9$ MeV for the η_b signal.

To confirm that this state is identical to the state observed in the $\Upsilon(3S) \to \gamma\eta_b$ analysis [1] we calculate the significance of the signal with the signal peak fixed to 614.3 MeV, the value expected for an η_b mass of 9388.9 MeV. The η_b signal significance is estimated as $\sqrt{\chi^2(\text{no signal}) - \chi^2(\text{fixed mass})}$, where $\chi^2(\text{fixed mass})$ is the χ^2 of the fit with the η_b signal included and $\chi^2(\text{no signal})$ is the χ^2 of the fit with the η_b PDF removed. The statistical significance estimated in this way is 3.7 standard deviations. The significance of the signal, including systematics, is estimated by making the variations discussed above. Additional cross-checks are performed by changing the lower (upper) limit of the fit range to 250 MeV (850 MeV) and varying the selection on $|\cos(\theta_T)|$. In all fits, the significance lies between 3.0 and 4.3 standard deviations.

The η_b mass derived from the E_γ signal is $M(\eta_b) = 9394.2^{+4.8}_{-4.9} \pm 2.0$ MeV/c^2. Using the PDG value of 9460.3 ± 0.3 MeV/c^2 for the $\Upsilon(1S)$ mass, we determine the $\Upsilon(1S)$-η_b mass splitting to be $66.1^{+4.9}_{-4.8} \pm 2.0$ MeV/c^2.

For the measurement of the branching fraction, we have an additional source of uncertainty resulting from the signal selection efficiency. The systematic uncertainty on the photon detection efficiency is 1.8%. We estimate the uncertainty on the hadronic selection efficiency (4.9%) by comparing data and MC efficiencies of the selection on hadronic $\Upsilon(1S)$ events. The uncertainty in photon quality selection efficiency (0.5%) is estimated from π^0 decays in data and MC. The difference between the efficiency in MC and the efficiency for a flat distribution (0.6%) is used as the uncertainty on the $|\cos\theta_T|$ selection. We determine the uncertainty for the π^0 selection (4.1%) by comparing the efficiency-corrected $\chi_{bJ}(1P)$ yield with and without the π^0 veto. The total systematic error on the selection efficiency is 6.7%. The uncertainty on the number of $\Upsilon(2S)$ events is 0.9%. Incorporating these systematic uncertainties, we determine the branching fraction of the decay $\Upsilon(2S) \to \gamma\eta_b$ to be $(3.9 \pm 1.1^{+1.1}_{-0.9}) \times 10^{-4}$.

In the $\Upsilon(3S)$ analysis [1], we estimated the systematic uncertainty on the signal efficiency using $\chi_{bJ}(2P)$ decays, incurring a large error (22%) due to the uncertainties in the $\chi_{bJ}(2P)$ branching fractions. The uncertainty in $\Upsilon(3S) \to \gamma\eta_b$ efficiency obtained using the procedure described above is 5.5%, resulting in a final branching fraction of $\mathcal{B}[\Upsilon(3S) \to \gamma\eta_b] = (4.8 \pm 0.5 \pm 0.6) \times 10^{-4}$. This value supersedes our previous result, which differs only in having a systematic uncertainty two times larger.

Using the results given above, we determine a branching fraction ratio of $\mathcal{B}[\Upsilon(2S) \to \gamma\eta_b]/\mathcal{B}[\Upsilon(3S) \to \gamma\eta_b] = 0.82 \pm 0.24^{+0.20}_{-0.19}$. The systematic uncertainties due to selection efficiency and the unknown η_b width partially cancel in the ratio. Our measurement is consistent with some of the theoretical estimates of this ratio of magnetic dipole transitions to the η_b, $0.3 - 0.7$ [2], while the absolute transition rates are not well-predicted by theoretical models.

In conclusion, we have obtained evidence, with a significance of 3.0 standard deviations, for the radiative decay of the $\Upsilon(2S)$ to a narrow state with a mass slightly less than that of the $\Upsilon(1S)$. The ratio of the radiative production rates for this state at the $\Upsilon(2S)$ and $\Upsilon(3S)$ resonances is consistent with that expected of the η_b. Under this interpretation, the mass of the η_b is $9394.2^{+4.8}_{-4.9} \pm 2.0$ MeV/c^2, which corresponds to a mass splitting between the $\Upsilon(1S)$ and the η_b of $66.1^{+4.9}_{-4.8} \pm 2.0$ MeV/c^2, consistent with the value from the $\Upsilon(3S)$ analysis. The aver-

age of the two results is $M(\eta_b) = 9390.8 \pm 3.2$ MeV/c^2. This value of the η_b mass is consistent with a recent unquenched lattice prediction [5] but more than two standard deviations away from the mass predicted by approaches based on perturbative QCD [14].

---

[*] Now at Temple University, Philadelphia, Pennsylvania 19122, USA

[†] Now at Tel Aviv University, Tel Aviv, 69978, Israel

[‡] Also with Università di Perugia, Dipartimento di Fisica, Perugia, Italy

[§] Also with Università di Roma La Sapienza, I-00185 Roma, Italy

[¶] Now at University of South Alabama, Mobile, Alabama 36688, USA

[**] Also with Laboratoire de Physique Nucléaire et de Hautes Energies, IN2P3/CNRS, Université Pierre et Marie Curie-Paris6, Université Denis Diderot-Paris7, F-75252 Paris, France

[††] Also with Università di Sassari, Sassari, Italy

[1] B. Aubert *et al.* (*BABAR* Collaboration), Phys. Rev. Lett. **101**, 071801 (2008); **102**, 029901(E) (2009).

[2] S. Godfrey and J. L. Rosner, Phys. Rev. D **64**, 074011 (2001); **65**, 039901(E) (2002), and references therein.

[3] M. Artuso *et al.* (CLEO III Collaboration), Phys. Rev. Lett. **94**, 032001 (2005).

[4] For a comprehensive review, see N. Brambilla *et al.* (Quarkonium Working Group), CERN Yellow Report, CERN-2005-005 (2005).

[5] A. Gray *et al.* (HPQCD and UKQCD Collaborations), Phys. Rev. D **72**, 094507 (2005); T. Burch and C. Ehmann, Nucl. Phys. **A797**, 33(2007); T.-W. Chiu *et al.* (TWQCD Collaboration), Phys. Lett. B **651**, 171 (2007).

[6] B. Aubert *et al.* (*BABAR* Collaboration), Nucl. Instrum. Methods Phys. Res., Sect. A **479**, 1 (2002).

[7] G. C. Fox and S. Wolfram, Nucl. Phys. **B149**, 413 (1979).

[8] A. Drescher *et al.* (ARGUS Collaboration), Nucl. Instrum. Methods Phys. Res., Sect. A **237**, 464 (1985).

[9] S. Brandt *et al.*, Phys. Lett. **12**, 57 (1964); E. Farhi, Phys. Rev. Lett. **39**, 1587 (1977).

[10] The *BABAR* detector Monte Carlo simulation is based on GEANT4: S. Agostinelli *et al.*, Nucl. Instrum. Methods Phys. Res., Sect. A **506**, 250 (2003); Simulated events are generated with Jetset 7.4: T. Sjöstrand and M. Bengtsson, Comput. Phys. Commun. **43**, 367 (1987).

[11] J. E. Gaiser, Ph.D. thesis, Stanford University [SLAC-R-255] (1982).

[12] C. Amsler *et al.* (Particle Data Group), Phys. Lett. B **667**, 1 (2008).

[13] W. Kwong, P. B. Mackenzie, R. Rosenfeld, and J. L. Rosner, Phys. Rev. D **37**, 3210 (1988); C. S. Kim, T. Lee, and G. L. Wang, Phys. Lett. B **606**, 323 (2005); J. P. Lansberg and T. N. Pham, Phys. Rev. D **75**, 017501 (2007).

[14] B. A. Kniehl *et al.*, Phys. Rev. Lett. **92**, 242001 (2004); S. Recksiegel and Y. Sumino, Phys. Lett. B **578**, 369 (2004).